HIGH CURRENT PERFORMANCE OF THE CERN PS LINAC

C. S. Taylor

CERN

1. INTRODUCTION

In April of this year we were able for the first time to accelerate more than 50 mA through the 50 MeV Linac injector of the CERN 25 GeV proton synchrotron. We have attempted since then to find out as much as possible about the behaviour of the Linac at these currents. The measurements reported below are mainly concerned with high currents but we have included for general interest some low current measurements of acceptance, and radial and longitudinal «memory» of transfer characteristics.

50 MeV in three separate tanks of 10, 30 and 50 MeV output energies respectively. The tanks are powered by individual high power triodes at 200 MHz and are pumped by mercury pumps. The machine is required for injection into the synchrotron in continuous runs of 11 days of 11 days or 258 h separated by 3 days of maintenance and test and in 1962 was responsible for 3.4% of loss of scheduled time due to faults, of which 1.6% was due to pre-injector troubles. The beam current growth over the years is summarised in Fig. 1, which also indicates summarily the causes of current increase.

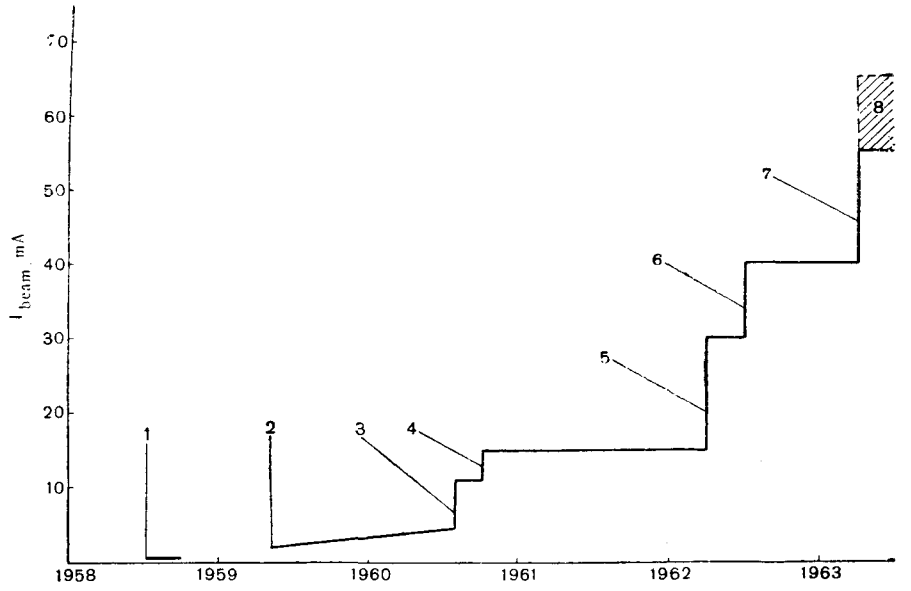

Fig. 1. Linac beam current growth over the years:
1 — grid focusing in Tank 1 (300 μA); *2* — installation of quadrupoles in Tank 1; *3* — buncher; *4* — modified electrode in acc. column; *5* — new triplets, variable voltage on outer electrodes of elect. lens; *6* — new source canal; *7* — rearrangement of focusing elements of prei-njector; *8* — present state.

2. HISTORY

The Linac machine is very much as it was reported in the Regenstreif reports [1, 2], the main changes being in the pre-injector, i. e. the source, the high tension engineering, and the 500 kV beam transport. As a brief reminder, the machine accelerates from 500 kV to

3. PRE-INJECTOR

We define the pre-injector as everything up to the input of the first Linac tank.

3.1. Ion Source [3,5]

The changes in the source chamber itself since the Regenstreif* description concern

* loc. cit.

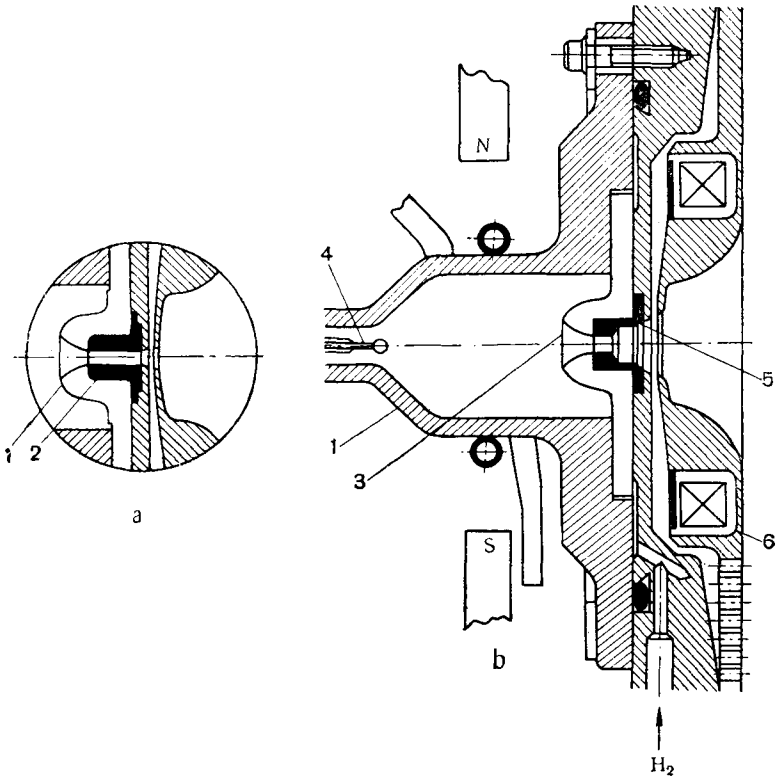

Fig. 2. RF ion source:
a — original source; b — modified source; *1* — glazed ceramic; *2* — outlet ⌀ 35, *l* = 10 mm; *3* — cathode shield (pyrex); *4* — anode (W); *5* — cathode (Ni), outlet ⌀ 4, *l* = 5 mm; *6* — beam current, transformer.

Source Characteristics

Max. beam current in labo: 220 mA. Present normal working current: 170—200 mA. Normal period between cleaning: 2 weeks (270 h). Proton percentage: $\frac{H_1}{\Sigma H_n}$ = 90%. RF — Power: 6—8 kW; 140 MHz. Approx. source pressure: 2×10^{-3} mm Hg.

fhe extraction canal length and diameter and the cathode protection which has been changed trom ceramic to pyrex. Fig. 2 shows the old and new chambers for comparison together with a summary of the present characteristics. The effect of the change in canal dimension is shown in Fig. 3. The increase in gas flow has not introduced any noticeable difficulties in the maintenance of adequate column pressure.

Emittance measurements have been carried out by drifting particles through a slitted aluminium plate on to photo-copying paper. The images produced by this technique both at source extraction energy and at 500 kV contain a fairly distinct «second spectrum» in addition to the primary pattern, indicating a discontinuity in the phase plane. This second spectrum appears to carry H_1^+, H_2^+ and H_3^+ ions in the same ratio as the main spectrum. Its formation is being studied at the moment. Fig. 4 shows the image of the slits on the photo-copying paper and the emittance surface derived from it. Fig. 5 shows the present appearance of the ion source block, of which there are five examples available for operation and experiment.

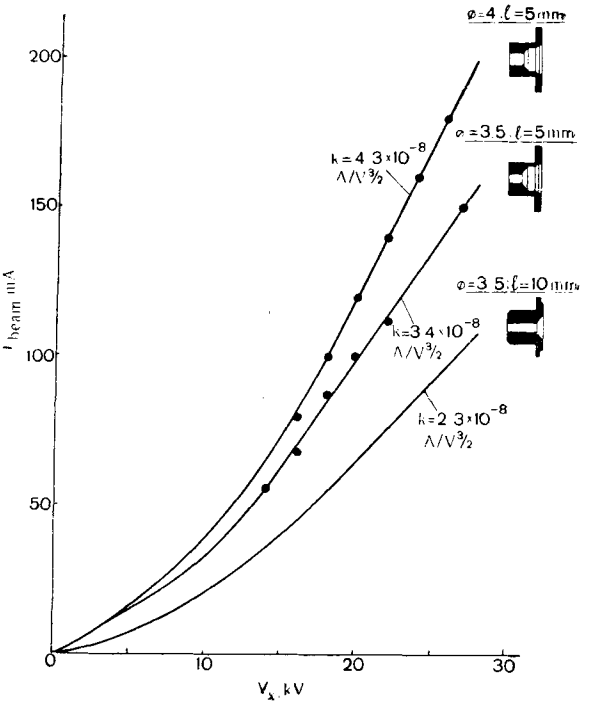

Fig. 3. RF ion source perveance curves. $I_{\text{beam}} = k \cdot V_x^{3/2}$.

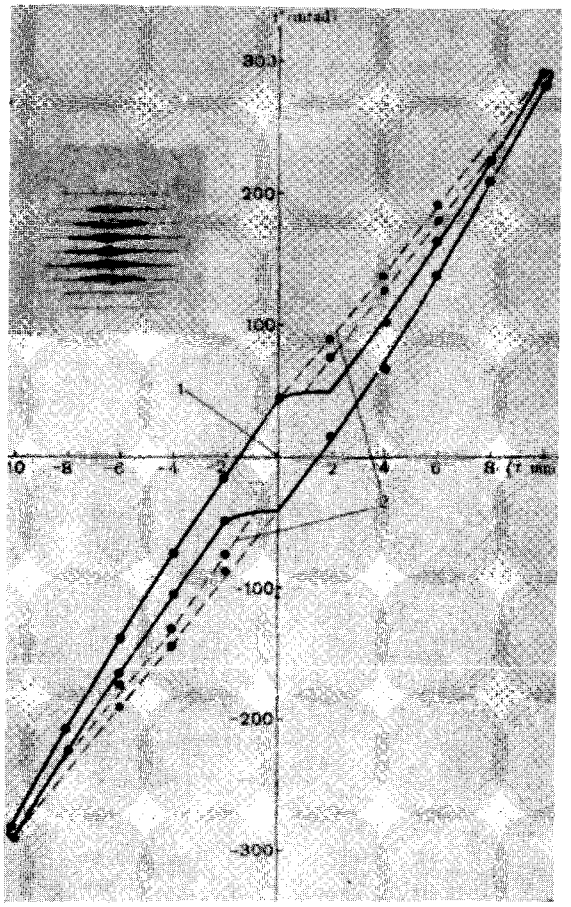

Fig. 4. RF ion source emittance:
1 — main beam; *2* — «second spectrum».

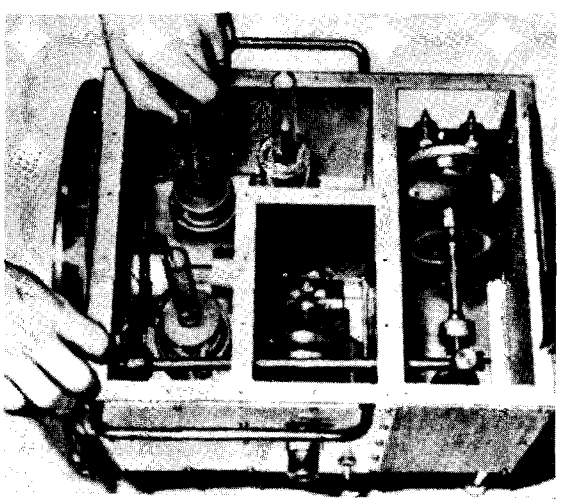

Fig. 5. Assembly of RF ion source.

3.2. Source to Linac Beam Transformer [4, 6]

From the source the beam is focussed by the three-electrode electrostatic lens to a neck near the earth end of the column after which it expands under the influence of its original divergence plus space charge forces to the first quadrupole triplet. A second triplet is placed fairly close to the Linac input. Recently both triplets were shifted as a result of trajectory calculations, and in fact the first triplet is now integral with the last electrode of the accelerating column.

Fig. 6 shows the general disposition of the elements and the currents at different points before and after the changes. Tests have been made with two types of electrostatic lens [4, 7] but in practice there seems to be little to choose between them. The effectiveness of both lenses however was improved by connecting a variable voltage to the outer electrodes instead of supplying them from the first 40 kV section of the column. One has gained in fact a degree of freedom in the matching problem, radius as well as focal length now being controllable.

Fig. 7 shows a typical emittance diagram at 500 kV measured at the end of the column. The general shape corresponds fairly well to the shape measured directly after the source, but not to the computed shapes. A computer programme is now being developed to solve Poisson's equation in place of the Laplacian solution with uniform charge density used hitherto [8, 9].

Fig. 8 shows how the 500 kV emittance increases with source current; the area in phase space is seen to rise approximately linearly over the range measured.

3.3. 500 kV Assembly

The present state of the column is indicated by the photograph of Fig. 9 and the electrical circuit shown in Fig. 10. It may be noted that the freon envelope described in Regenstreif* has been removed. This was made possible by a re-design of the voltage dividing resistors [10] and by holding the thin support pillar to a uniform field distribution by a spiral of carbon resistors wound around it. Normal operating current from the H. T. set [11] is 0.65 mA, 0.1 mA for the column resistive load, 0 to 20 μA corona current, and 0.55 mA for measuring and other devices. (See Fig. 10).

* loc. cit.

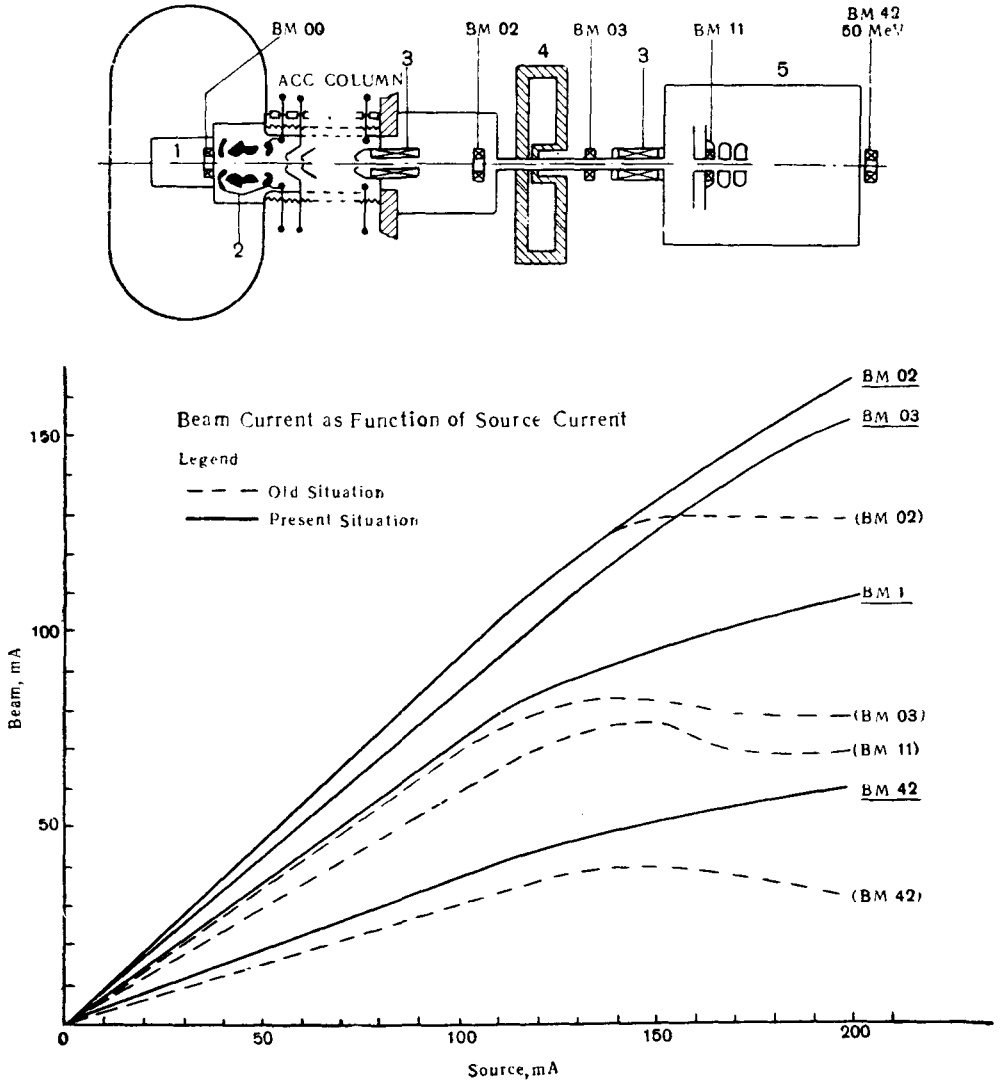

Fig. 6. Source to linac beam transport:
1 — ion source; *2* — electrostatic lens; *3* — triplet; *4*—buncher; *5* — linac.

With a beam pulse of 200 mA, the 500 kV terminal drops in voltage are 1 to 3.5 kV, depending on the amount of back streaming electrons. The effect of this energy change is referred to in Section 4.2.4. below. Radiation from the 500 kV assembly is <5 mR/h.

4. LINEAR ACCELERATOR

4.1. Radial Characteristics

In working with beams of particles one frequently wants to know how much beam current is lost if a certain amount of phase space is removed, for example by aperture limitation. It follows then that a useful working description of a beam should include the current density distribution across the phase space. In passing from beam properties to the question of how much beam a machine can accept we find an analogous problem of distribution, this time the distribution of the machine's ability to trap particles as we move across the phase space. In the following section we shall discuss this problem and its bearing on the measurement of acceptance before proceeding to the actual results.

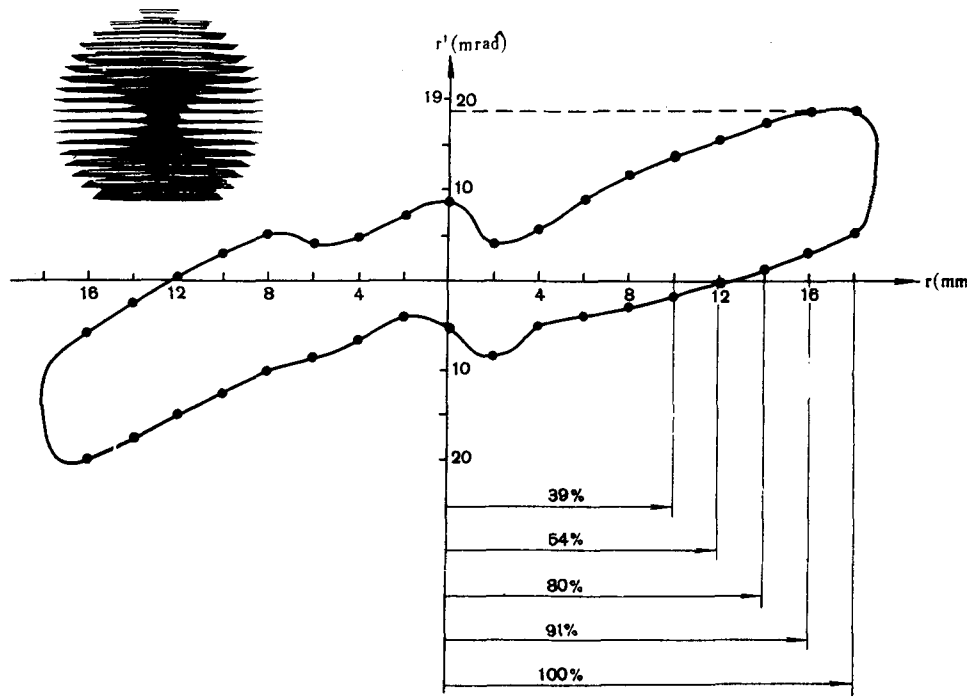

Fig. 7. 500 kV emmittance at 150 mA.

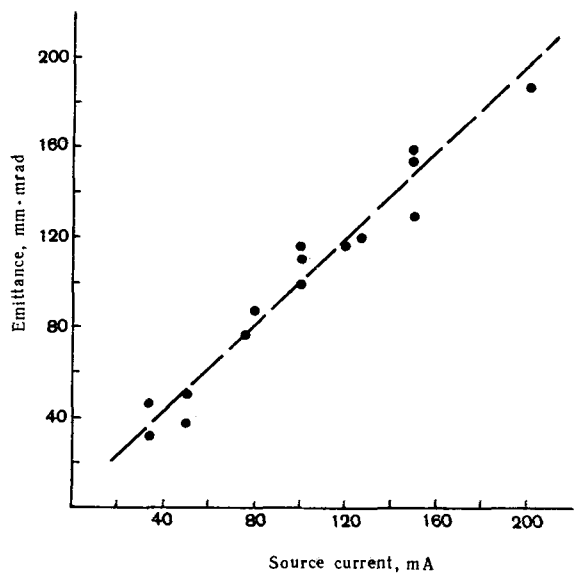

Fig. 8. Increase of emmittance with current.

4.1.1. Radial Acceptance

The radial acceptance of a linear accelerator has been shown to be strongly dependent on the phase of injected particles with respect to the stationary phase angle and several numerical computations of this effect have been carried out [12, 13]. Fig. 11 illustrates this phase dependence. It is evident that in the common area near the centre, the machine does not mind what phase the particles have, but away from the centre the machine becomes more and more selective, accepting smaller and smaller ranges of phases, and trapping with lower and lower efficiency, assuming that the full range of phases is injected at every point in the radial plane. This lower trapping away from the centre probably helps to account for the fact that measured overall capture efficiencies are usually less than predicted. Nevertheless these outer regions remain useful if one is interested in the total current accelerated rather than in high trapping efficiency.

We can measure the acceptance to a given bunched beam in say the horizontal plane by scanning the input phase space with a beam element defined by slits and recording at each point in the phase plane the «transmission» or ratio of output to input current. At the same time vertical motion should be limited so as to be always well within its acceptance.

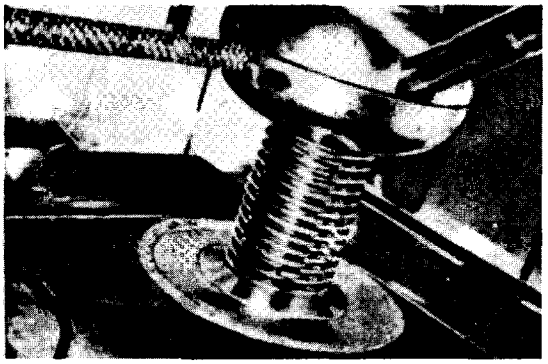

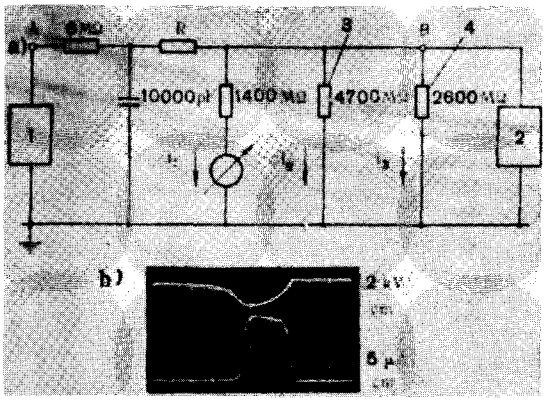

Fig. 10.

a) R = 10, 22, 45 kΩ for different voltage drops
i_1 = 360 μA
i_2 = 190 μA
i_3 = 105 μA
$i_1 + i_2 + i_3$ = 655 μA
i_{corona} = 0—20 μA
ΔU = 3.4 kV for R = 10 kΩ
6—9 kV for R = 45 kΩ
beam current ≃ 200 mA
1 — HT generator; *2* — accelerating column; *3* — resistance of column support; *4* — column voltage grading resistance.
b) Upper curve: voltage drop at point *B*.
Lower curve: beam current pulse in the accelerating column.

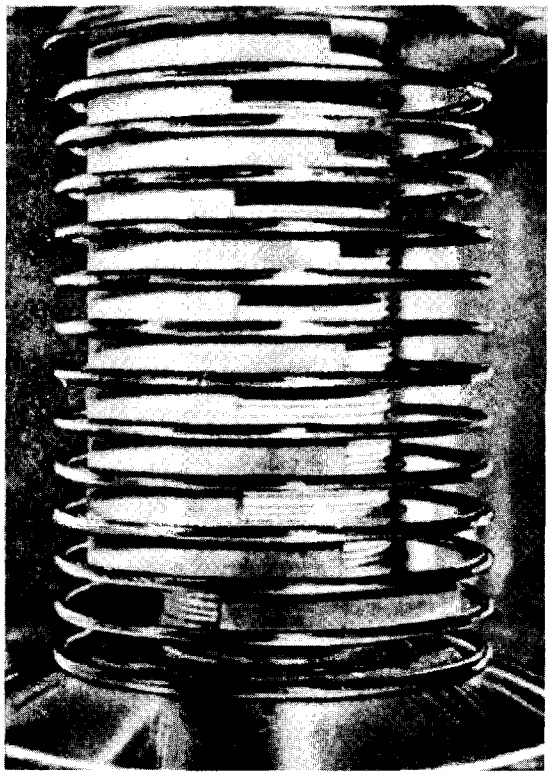

Fig. 9. 500 kV accelerating column.

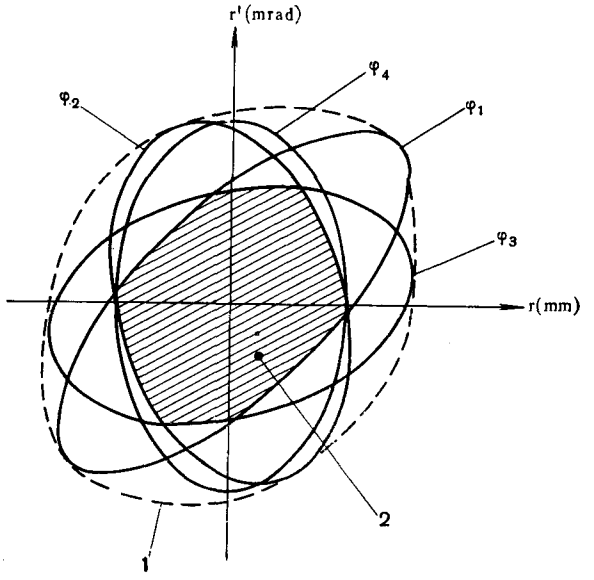

Fig. 11. Acceptance for different phase angles in injected beam:
1 — overall acceptance; *2* — common area

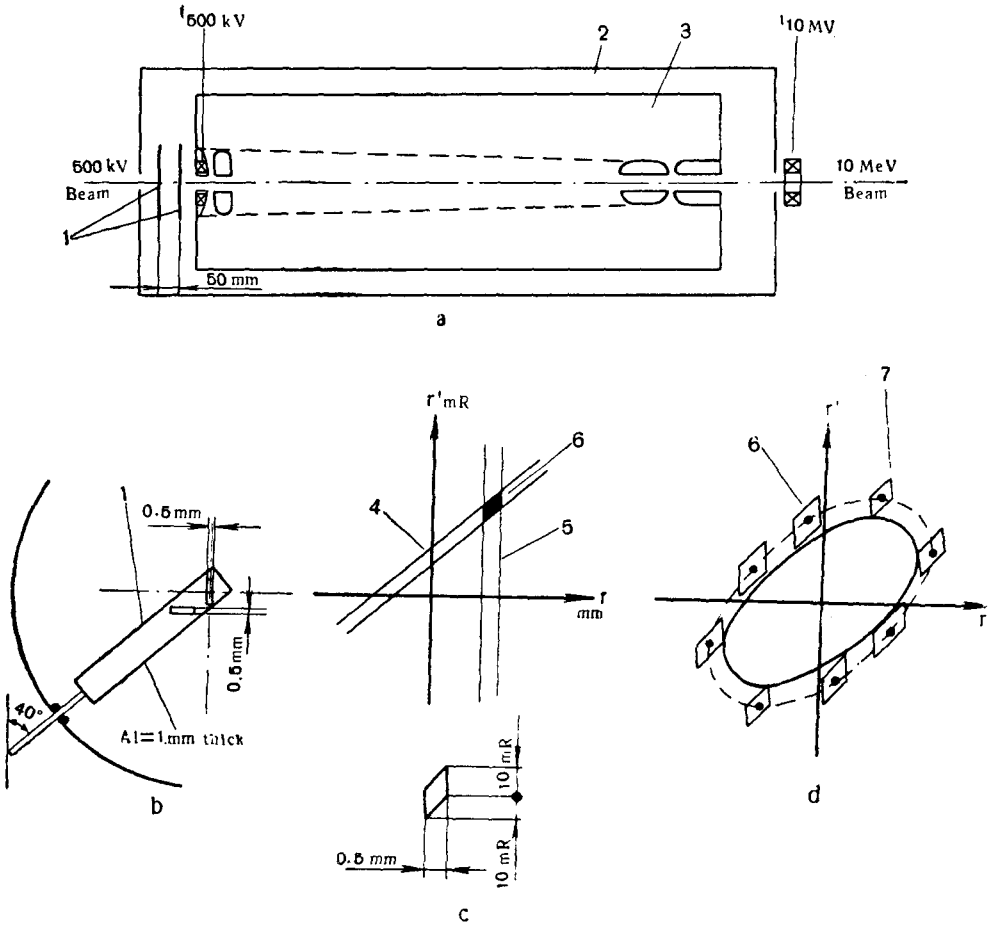

Fig. 12. Radial acceptance measurement:
a — general arrangement; *b* — arrangement of slider; *c* — radial phase plane of second slit; *d* — correction for finite size of beam element; *1* — identical sliders; *2* — vacuum envelope; *3* — cavity; *4* — first slit; *5* — second slit; *6* — beam element; *7* — element centers for $\frac{i_{10\,MV}}{i_{500\,kV}} = 5\%$.

A preliminary measurement of this type has been carried out recently [14], but for practical reasons there could only be limitation in one plane at a time so that the results could be seriously weighted by loss in the orthogonal plane. The principle of the measurement is shown in Fig. 12.

We measure transmission systematically across the phase plane and set the acceptance limits arbitrarily at a transmission of 0.05. Preliminary results are shown in Fig. 13 with, for comparison, the calculated ellipse for $\varphi = \varphi s = 30°$, $q = \frac{\omega r}{\omega \varphi} = 0.75$ and nominal energy. The question of whether the lack of agreement is mainly attributable to the orthogonal radial plane will have to wait until we can limit both planes simultaneously.

4.1.2. Emittance

The slotted plate and film method of emittance measurement has found its main use so far at source or column energy, but recently it was found possible to mount these elements between tanks at 10 MeV and some preliminary exposures have been made and analysed. For a 500 kV beam of 150 mm·mrad (or μrad) emittance we should expect 150 $\sqrt{\frac{0.5}{10}} = 35$ μrad at 10 MeV). In fact our measurements indicate 30% more, i. e. 45 μrad. These expe-

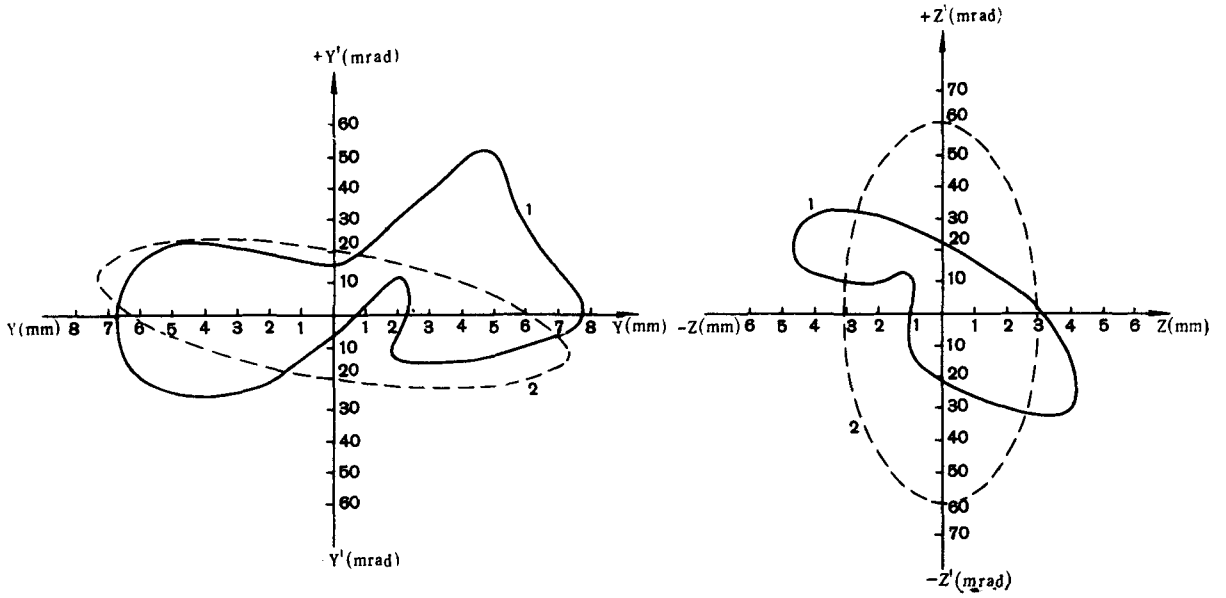

Fig. 13. Linac acceptances:
1 — measured acceptances; *2* — theoretical acceptances for $\varphi_S = 30°$, $q = 0.75$.

riments are being continued in order to ascertain the validity of the experimental method. At 50 MeV all measurements up to now have been made with various combinations of adjustable apertures and a lens [15].

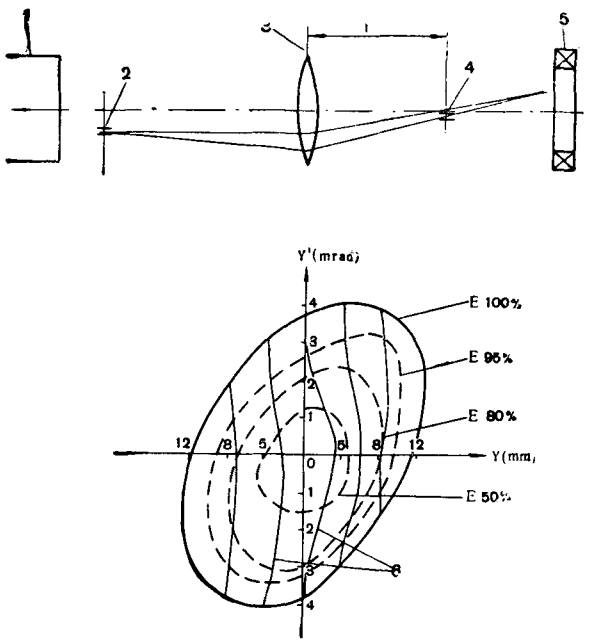

Fig. 14. Emittance measurement 50 MeV:
1 — linac; *2* — diameter slit; *3* — triplet; *4* — angle slit; *5* — current transformer; *6* — density distribution curves (1 mA).

From the distribution of current density with angle for different diameters (Fig. 14) one can plot contours of phase space current density and hence derive the proportion of total current within a given emittance. In practice it has been found that the diagrams remain approximately as ellipses in principal axes and hence a quick measurement of total extension in angle and diameter gives a good idea of total emittances.

It is interesting to note that with the debuncher assuring a good energy spread this measurement has on occasion been the first indication of trouble in the longitudinal plane, for example incorrect levels or phases due to changed loops or mal-functioning instruments or line lengtheners, etc. No systematic measurements have yet been carried out on the dependence of radial motion on phase motion.

Fig. 15 shows emittance diagram at 55 mA for both planes. The 100% emittances are 46 μrad for the horizontal plane and 48 μrad for the vertical plane. The derived curve of percentage current against percentage emittance is also included in Fig. 15 and illustrates how inefficient is the outer portion of the beam. In general the diagrams have been found to be approximately elliptical, the contours

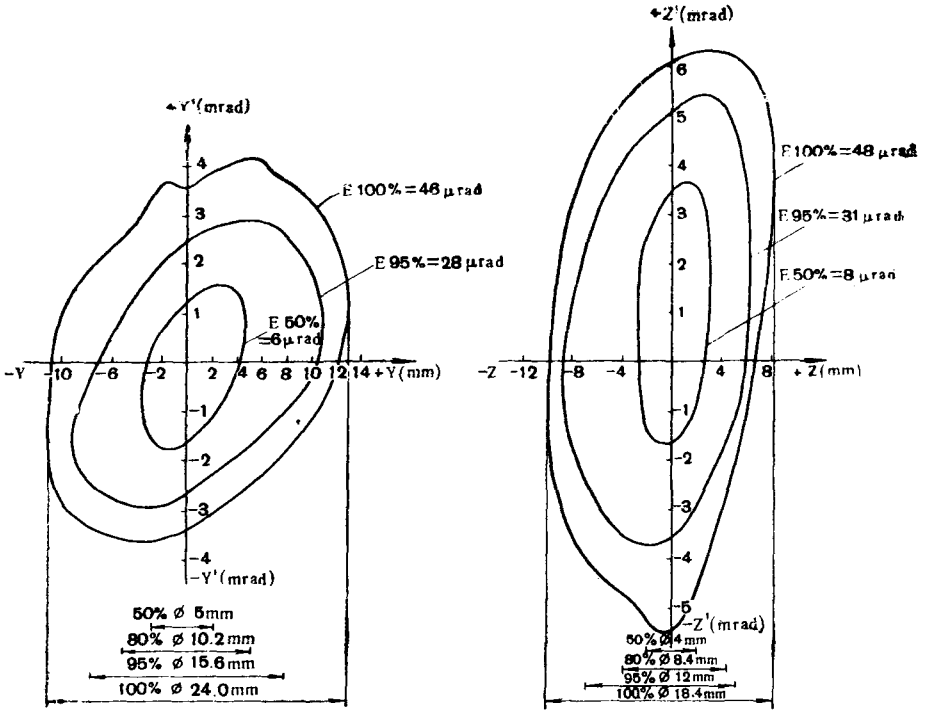

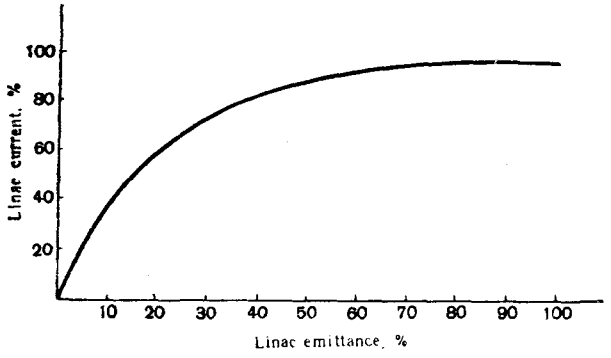

Fig. 15. Linac emittances.

concentric, and the distribution Gaussian. Since the slotted plate and film method has not yet been extended to 50 MeV no direct comparison between measurements at low and high energies is possible, but is fairly certain that the emulsion is more sensitive than the beam transformers, and present 50 MeV figures are probably on the low side. If we take 50 μrad as a minimum figure for 100% beam we have an overall ratio between the 50 MeV emittance and the transformed 500 kV emittance of $\frac{50}{15.0}$ or 3.3.

4.1.3. Radial Transfer Characteristics

The installation of the 500 kV acceptance measuring slits enables us to define beam elements in the linac input radial phase plane, and the properties of these elements can then be studied at 50 MeV by means of the apertures, lens and transformers. This study was suggested by the observed steering effect of the 500 kV steering coils on the 50 MeV beam. Preliminary measurements show that our small element (5 μrad) in the centre of the 500 kV beam emittance occupies more than 50 times its transformed area in phase space at 50 MeV.

4.2. Longitudinal Characteristics

4.2.1. Energy Acceptance

The acceptance of the Linac at various tank levels has been measured as a function of injection energy. For this purpose the beam was collimated to 5 mm to reduce radial effects and beam loading; the buncher was switched off. The results, shown in Fig. 16, demonstrate a shift of the maximum trapping towards higher input energies, with the tank level increased. The optimum trapping lies at an input energy above the nominal value of the centre of the ideal RF bucket, as described in reports by R. Taylor [16] and J. P. Blewett [17]. The injected energy was precisely measured with recently recalibrated instruments [18].

4.2.2. Energy Spread

Energy spread at high currents has been less of a problem than was feared. Typically it is less than ± 150 kV, in < ± 3‰ with the debuncher. Even without the debuncher working, the spread is of the order of ± 300 kV. There is however a shift of the mean energy during the beam pulse, revealed by scanning the analysed image with a narrow slit and measuring the current passing through the slit at the beginning, middle and end of the beam pulse. Fig. 17 shows this effect with the debuncher disconnected. We know that there are two possible causes of this, tank beam loading and 500 kV column beam loading. We shall describe in the next section the effect of column loading in the 50 MeV beam or the energy transfer characteristics of the accelerator.

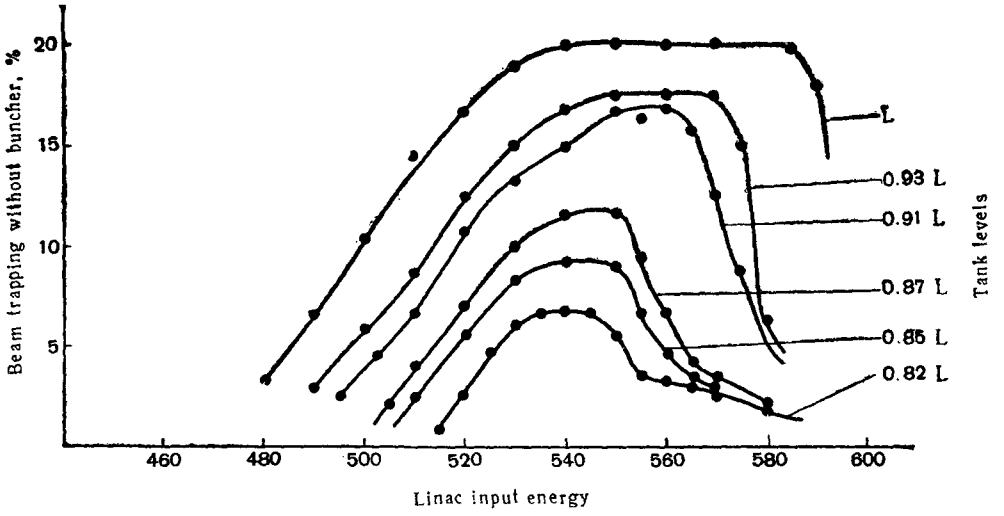

Fig. 16. Linac trapping as function of input energy.

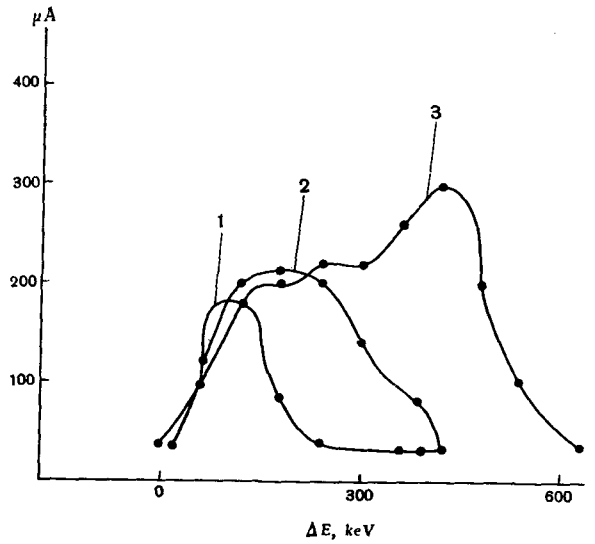

Fig. 17. Shift of mean energy during beam pulse: *1* — beginning; *2* — middle; *3* — end.

4.2.3. Energy Transfer Characteristics

Since we have no method of defining a beam element in the longitudinal phase space by both co-ordinates, we may only vary the input energy without buncher and measure the change n output energy. Fig. 18 shows the measured upper and lower energy limits of the 50 MeV beam as a function of input energy with the beam again collimated to reduce RF beam loading and without the buncher or debuncher. For comparison we show in Fig. 19 the results obtained when the buncher is connected at a fixed phase.

4.2.4. RF Beam Loading

A simplified analysis of the fall in accelerating field can be made by assuming that the energy required to accelerate the beam will come entirely from the stored energy of the cavity. In the first tank for example, with approximately 30 J stored in the steady state and 5 J required by a 50 mA beam, the stored energy must fall by 15% and the field by about 7%. Measurements show that this approach is reasonably valid. Fig. 20 shows the accelerating field drop in each cavity as a function of accelerated current. This effect can be compensated by an increase in RF power during the passage of the beam, i. e. by modulating the supply [19, 20]. Calculation indicates a phase change of a degree or so at 50 mA and rough measurements confirm the order of magnitude.

5. GENERAL

5.1. Stability

The influence of different parameters on the Linac performance is being studied on a statistical basis. The parameters are transfered on to punched tapes by means of data logging equipment [21], and these tapes are then directly fed into and analysed by a digital

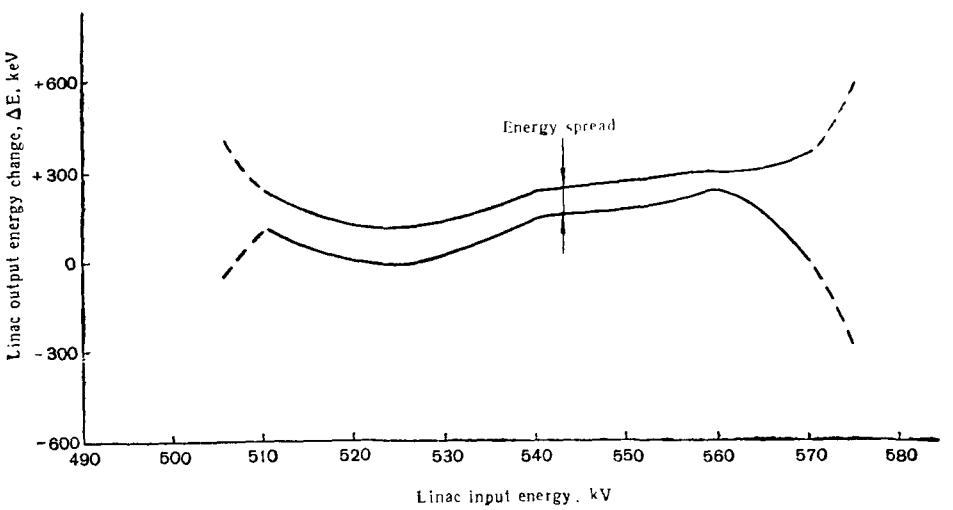

Fig. 18. Energy change at linac output as function of input energy (beam reduced to 1.5 mA, buncher and debuncher disconnected).

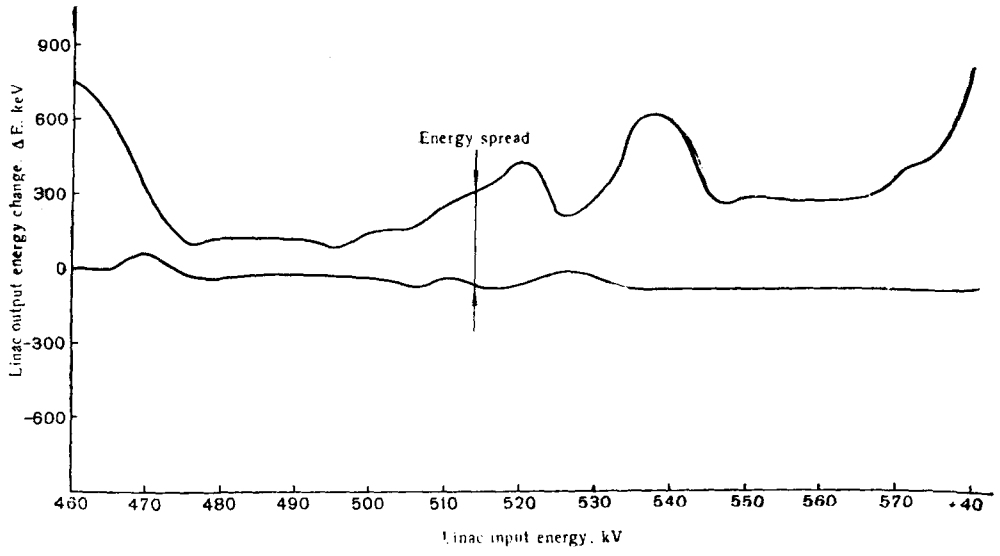

Fig. 19. Energy change at linac output as function of input energy (1.5 mA, buncher on, debuncher disconnected).

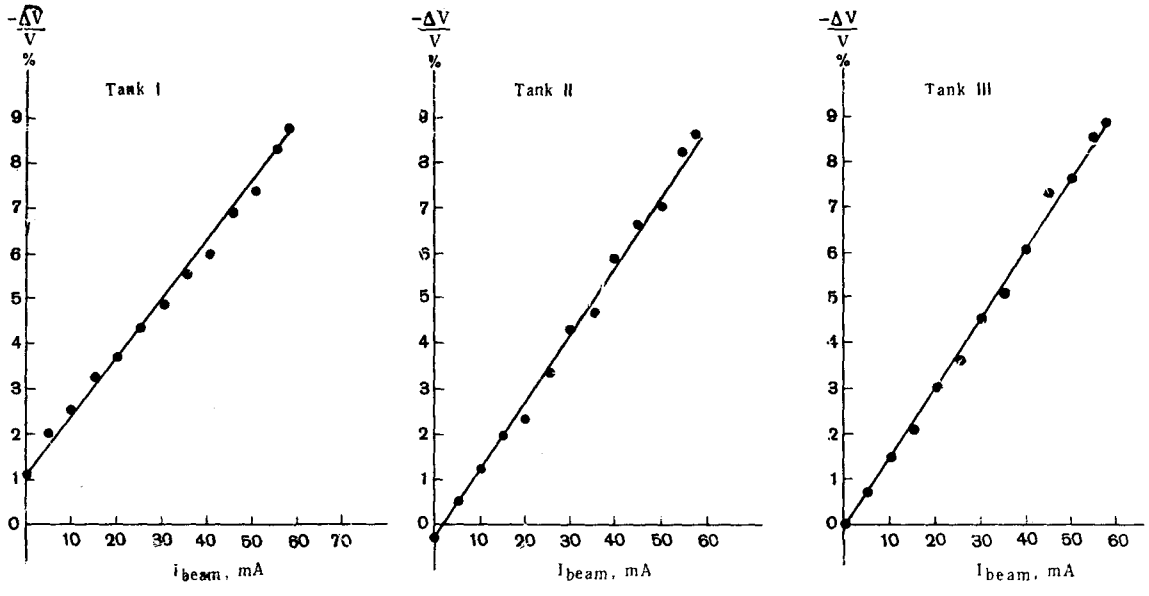

Fig. 20. Tank voltage drops as function of beam intensity.

computer. Fig. 21 shows the histogram for the pre-injector beam current variations during a run of 223 pulses. The standard deviation

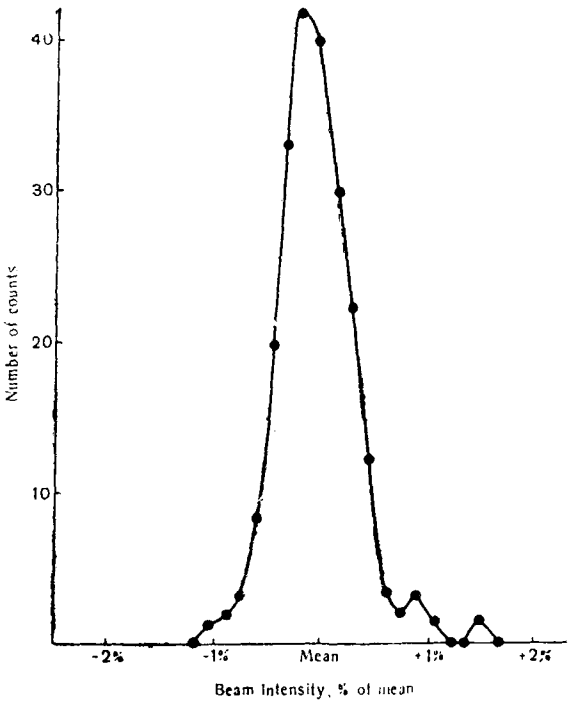

Fig. 21. Histogram of pre-injector beam intensity — BMO2 (223 pulses at 1.5 s repetition).

is 0.34% of the mean. Computer programmes have been prepared already for power spectra and multiple regression analyses [22].

5.2. Radiation

Radiation has not proved a serious problem with the Linac. Initially, a closed area was defined by barriers and interlocked doors, and the positions of these have not had to be modified. During early surveys it was found that when the beam was correctly accelerated levels were low enough to allow access, providing no appreciable beam loss occurred. A monitor was installed to take advantage of the situation, but the large increase in beam current caused the use of this system to be suspended. The present situation (with a normal beam of about 50 mA pulse current) is that radiation levels are between 10 and 150 mrem/h in the closed area under normal running conditions. Should the beam be stopped (e. g. by closing a vacuum valve) or even defocussed, the levels become very much higher. Normally, no access for personnel is allowed whenever beam is accelerated above 500 keV. During all normal operation, radiation outside the security barriers remains below permissible levels (taken as 2.5 mrem/h). Induced activity in accelerator components has also remained low in the Linac itself, and has not seriously hindered repairs and modifications.

5.3. Conclusion

Since 1959 the principal task of the Linac Group has been to supply the CPS with as intense a beam as possible. The emphasis is now, changing from beam intensity to beam density in the phase plane. With care we can produce 50 mA circulating without loss for 3 turns of the PS but to increase this we shall have to get more current into the useful inner regions of the radial emittances. At the moment the pre-injector seems to be the most profitable line of approach. Finally it is almost certain that progress beyond the 50 mA circulating beam will require a considerable refinement of instrumentation and measurement throughout the machine.

REFERENCES

1. Regenstreif E. The CERN Proton Synchrotron, Part 2, CERN 60-26.
2. Regenstreif E. The CERN Proton Synchrotron, Part 3, CERN 62-3.
3. Tallgren U. Recent Experiments and Measurements on the CPS Ion Source, CERN Internal Report, MPS/Int. LIN 62-3.
4. Sluyters Th. CPS Pre-injector Measurements, CERN Internal Report, MPS/Int. LIN 63-6.
5. Tallgren U. The Formation of Phase Space Areas and the Influence of Space Charge on the Emittance of the CPS RF Ion Source, CERN Internal Report. (To be published.)
6. Weiss M. Considerations on the Beam Transport System of the Pre-injector for the 50 MeV Linac, CERN Internal Report, MPS/Int. LIN 63-3.
7. Septier A. Aberration sphérique de quelques lentilles électrostatiques à symétrie de révolution pour des faisceaux de grande ouverture, CERN 60-39.
8. Hornsby J. S. A Computer Programme for the Solution of Elliptic Partial Differential Equations (Potential Problems), CERN 63-7.
9. Weiss M. Considerations of the Beam Transport System of the Pre-injector for the 50 MeV Linac, Second Part. (To be published.)
10. Dubois R. Chaines résistives de la colonne accélératrice du Linac, CERN Internal Report, MPS/Int. LIN 63-2.
11. Huguenin J. Pannes et réparations du générateur 600 kV du Linac, CERN Internal Report, MPS/Int. LIN 62-5.

12. Hereward H. G., Johnsen K. CERN Symposium, 1956, p. 167—172.
13. Cohen D. Radial Motions in the 50 MeV Linear Accelerator, ANLAD-57.
14. Têtu P. Mesures d'acceptance du Linac. CERN Internal Report. (To be published.)
15. Têtu P. Emittance du faisceau Linac, CERN Internal Report, MPS/Int, LIN 63-5.
16. Taylor R. Acceptance of Axially and Radially Oscillating Particles in the Linac Injector for the Harwell 7 GeV Proton Synchrotron (NIMROD) AERE-R30B.

DISCUSSION

L. C. Teng

1. How stable is your emittance figure. We find that the shape of our emittance figure changes from day to day.

2. Could you say something about the dependence of the emittance area on the current?

C. S. Taylor

1. Fairly stable. If it is found to be very different from the usual figure we start looking for the causes.

2. We haven't much information about this at 50 MeV but we can say that up till now more pre-injector current has meant more emittance into the linac, and this has meant more out. There is negligible loss after trapping.

A. van Steenbergen

May I comment on this. At BNL we have done several accurate measurements of Linac emittance and found that considering 90% of a total beam of 24 mA the emittance was about a factor of 2 larger than the emittance of a 12 mA beam, again considering 90% of the total beam.

I. M. Kapchinskiĭ

Did you measure the beam cross section at different points along the accelerator? What can you say about the nature of the envelope along the axis? Is the envelope almost periodic?

C. S. Taylor

Besides measurements at the input and output of the accelerator, we have recently been able to measure emittance between the first and second tanks, is at 10 MeV. That is as far as we' ve been able to go into this question.